A Simple Thermodynamical Theory for Dust Devils

NILTON O. RENNÓ, MATTHEW L. BURKETT, AND MATTHEW P. LARKIN

Department of Atmospheric Sciences, The University of Arizona, Tucson, Arizona

(Manuscript received 7 February 1997, in final form 23 January 1998)

ABSTRACT

Based on the heat engine framework, a simple scaling theory for dust devils is proposed and compared to observations. This theory provides a simple physical interpretation for many of the observed characteristics of dust devils. In particular, it predicts the potential intensity and the diurnal variation of dust devil occurrence. It also predicts that the intensity of dust devils depends on the product of two thermodynamic efficiencies, corresponding respectively to vertical and horizontal temperature gradients.

1. Introduction

Dust devils are low pressure, warm-core vortices with typical surface diameters between 1 and 50 m. Since they receive their vorticity from local wind shears that can be either due to the convective circulation itself or due to larger-scale phenomena, they rotate either cyclonically or anticyclonically with equal probability (Williams 1948; Sinclair 1966; Carroll and Ryan 1970). Dust devils are more frequently observed in hot desert regions, although they have been observed in colder regions such as the subartic (Wegener 1914; Grant 1949). To a first approximation, a dust devil moves with the speed of the ambient wind, typically at about 5 m s^{-1}. In general, dust devils slope with height in the wind shear direction. In environments of high wind speed ($\gtrsim$10 m s^{-1}), dust devil diameters are biased toward large values. About 55% of the dust devils observed around Tucson, Arizona, have diameters between 3 and 15 m, and 15% have diameters larger than 15 m (Sinclair 1966, 1969, 1973).

Figure 1 is a sketch of a dust devil. Near the surface, the warmest air parcels are spiraling in toward the moving dust devil while they absorb heat from the surface. Over the desert, the typical temperature and pressure perturbation observed within dust devils varies from 4 to 8 K and from 2.5 to 4.5 hPa (Sinclair 1973). The vertical velocity reaches positive peak values in the region of maximum temperature. A weaker and cooler downdraft, in nearly solid body rotation, is present in the dust devil core (Sinclair 1966, 1973; Kaimal and Businger 1970). The near-surface vertical velocity reaches peak values of about 15 m s^{-1} (Sinclair 1973; Ives 1947). Weak thermal updrafts and small dust devils are frequently observed in the wake of larger dust devils. The low-level tangential velocity also reaches peak values of about 15 m s^{-1}, while the near-surface radial velocity usually does not exceed 5 m s^{-1}. The radial velocity reaches its peak value outside the region of maximum tangential and vertical velocities (Sinclair 1973). Indeed, the radial velocity nearly vanishes in the region of maximum tangential wind. Moreover, since dust devils are warm-core vortices, the pressure perturbation and therefore the tangential velocity reach peak values a few meters above the ground and rapidly decrease with height. In fact, in typical dust devils the perturbation pressure value nearly vanishes just a few hundred meters above the surface.

Dust devils have tangential velocity profiles characteristic of a Rankine vortex. Moreover, to a first approximation, their tangential winds are in cyclostrophic balance above the surface. However, since there is a radial inflow of air toward their center, the observed pressure gradients are larger than those necessary to support cyclostrophic tangential winds (Sinclair 1973). Substantial mixing and expansion of the dust devil vortex occurs near the surface. Warm, near-surface air moves horizontally toward the low pressure center until it reaches the dust column. Then, it rises rapidly. Within the dust column, the radial velocity nearly vanishes. The presence of dust particles in the dust devil inner core is suppressed by both a descending motion and centrifugal forces (Sinclair 1966, 1973).

There is mounting evidence that dust devils form in the bottom of convective plumes (Battan 1958; Sinclair 1966; Ryan and Carroll 1970). The radial inflow of near-surface warm air into the rising plume results in the concentration of ambient vorticity and may lead to the establishment of a weak vortex. As the convective

Corresponding author address: Dr. Nilton O. Rennó, Department of Atmospheric Sciences, The University of Arizona, P.O. Box 210081, Tucson, AZ 85721-0081.
E-mail: renno@soar.atmo.arizona.edu

© 1998 American Meteorological Society

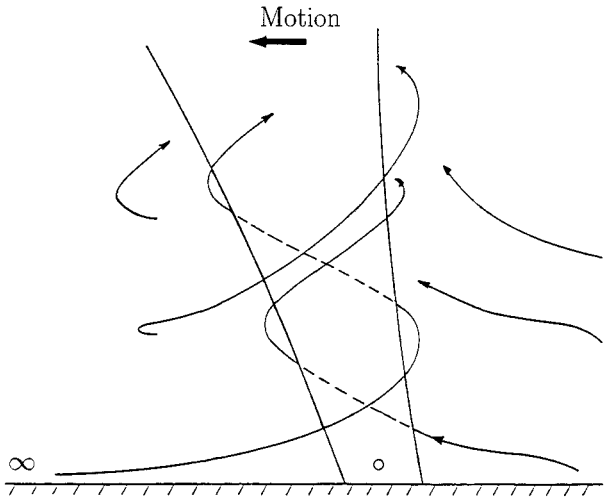

FIG. 1. Sketch of a dust devil (adapted from Sinclair 1966).

plume rises to higher altitudes, the pressure depression at its base increases. This low pressure center near the surface forces a spiral inflow of warm boundary layer air into the incipient dust devil. (Surface friction plays an important role in forcing this near-surface convergence of warm air.) When the surface is composed of loose materials, dust particles might become airborne making the dust devil visible. Thus, when loose materials are not present, intense vortices may exist and may not be visible to the observer. The intensity of a dust devil depends on the depth of the convective plume and the existence of local wind shears. When a dust devil crosses cold terrain, the dust column is cut off, and the convective plume quickly dissipates (Sinclair 1973).

The height of the dust column of a dust devil rarely exceeds 1 km. However, the thermal updraft above the dust devils (their invisible part) usually extends to the top of the convective layer. In the summertime, the convective boundary layer extends to about 3–4 km above the ground over the desert regions. The dust devil occurrence increases abruptly from nearly zero at around 1000 Mountain Standard Time (MST) to its maximum value at around 1300 MST (Sinclair 1969; Flower 1936; Williams 1948). Then, the dust devil activity slowly decreases as the afternoon progresses. In this study, we present a simple physical explanation for this distribution and for the potential intensity of dust devils.

Our main objective is to propose a simple scaling model for the potential intensity of dust devils. In order for a dust devil to form, both thermodynamical processes responsible for maintaining a pressure depression and dynamical processes capable of producing vorticity must be present. The various dynamical processes capable of producing and enhancing vertical vorticity in convective systems have been extensively studied in the atmospheric science literature (Lilly 1982; Davies-Jones 1984; Rotunno and Klemp 1985; Fiedler and Rotunno 1986; Simpson et al. 1986). We do not discuss these mechanisms in this paper. Instead, we focus on the thermodynamics of the convective process responsible for the maintenance of the pressure depression within a dust devil.

2. Dust devils as convective heat engines

Heat engines are devices that convert heat into mechanical energy. Therefore, any natural convective phenomenon is a heat engine. Emanuel (1986) and Rennó and Ingersoll (1996) idealized hurricanes and atmospheric convection as heat engines. In this study we use the framework developed by Emanuel (1986) and Rennó and Ingersoll (1996) to formulate a scaling theory for dust devils. We assume a dust devil in quasi-steady state. Since for a given set of environmental conditions a steady state is achieved only when the work done by the heat engine is balanced by mechanical friction, the quasi-steady state assumption implies that we aim at a theory for the maximum bulk thermodynamical intensity of a vortex in cyclostrophic balance. Therefore, the reader should be cautioned that our theory does not attempt to predict the upper bound for the maximum windspeed in a supercritical end-wall vortex. Fiedler and Rotunno (1986) showed that the thermodynamic speed limit can be exceeded at the foot of intense end-wall vortices.

We assume that most of the heat input to a dust devil heat engine is in the form of sensible heat flux at the surface, and that the heat output is in the form of thermal radiation emitted by subsiding air parcels. Moreover, we assume that the convective drafts are adiabatic and that the heat engine cycle is reversible. The available energy lost by the higher-entropy updraft air through mixing with the lower-entropy ambient air is implicitly included in our model through the definition of the cold temperature [see section 4 and Fig. 3 of Rennó and Ingersoll (1996) for a more detailed discussion of this issue].

An energy equation for a convecting air parcel follows from the dot product of the velocity vector with the equation of motion (Haltiner and Martin 1957). The resulting equation states that following an air parcel in steady state

$$d\left(\frac{1}{2}|\mathbf{v}|^2 + gz\right) + \alpha dp - \mathbf{f}\cdot d\mathbf{l} = 0, \qquad (1)$$

where $\mathbf{v}$ is the vector velocity, g the gravity acceleration, z the height above a reference level, α the specific volume, p the pressure, $\mathbf{f}$ the frictional force per unit mass, and $d\mathbf{l}$ an incremental distance along the air parcel's path.

Mass conservation requires that in steady state the circulations within a material volume occupied by the convective system must be closed in a frame of reference moving with the material volume [that is $\nabla\cdot(\rho\mathbf{v}) = 0$]. Thus, integrating Eq. (1) over mass on this material volume, we get

$$\int_m \alpha \, dp = \int_m \mathbf{f} \cdot d\mathbf{l}. \tag{2}$$

The notation $\int_m$ indicates an integral over mass on the entire material volume occupied by the convective system normalized by its mass.

The first law of thermodynamics applied to moist air can be written as

$$T \, ds = d(c_p T + L_v r) - \alpha dp, \tag{3}$$

where T is the absolute temperature, s the specific entropy, c_p the heat capacity at constant pressure per unit mass, L_v the latent heat of vaporization of water per unit mass, and r the water vapor mixing ratio. Integrating Eq. (3) over mass in the material volume occupied by the dust devil convective system in steady state, we get

$$\int_m T \, ds = -\int_m \alpha \, dp = \int_m p \, d\alpha, \tag{4}$$

where we have used the ideal gas law. It is important to recall that the integral of the exact differential over the material volume vanishes because the flow is steady, and in this case the vector $\rho\mathbf{v}$ has zero divergence. Equation (4) states that in steady state the work done by the convective system is equal to the net heat input into the convective heat engine. When the left-hand side of Eq. (4) is integrated over a Carnot cycle it represents the area enclosed by the hot and the cold adiabats (s_2 and s_1) and the hot and the cold isotherms (T_h and T_c), respectively, at the bottom and at the top of a ''Carnot convective circulation.'' This area, in turn, represents the total amount of work done by a convective cycle (Rennó and Ingersoll 1996). Brunt (1941) showed that, for a Boussinesq system, the area enclosed by the hot adiabatic, the ambient temperature sounding, and the top and the bottom of the convective layer represents the total amount of work done by the buoyancy forces in moving an air parcel along the updraft (that is convective available potential energy or CAPE). Equation (4) is more general because it also includes the work done by non-Boussinesq terms (e.g., the anelastic term).

It follows from Eqs. (2) and (4) that

$$\int_m T \, ds = -\int_m \mathbf{f} \cdot d\mathbf{l}. \tag{5}$$

This is not a new result; Eq. (5) simply states that, in steady state, the net work performed by the dust devil convective heat engine balances the frictional loss of energy. Alternatively, Eq. (5) can be expressed as a line integral around the convective cycle:

$$\oint T \, ds = -\oint \mathbf{f} \cdot d\mathbf{l}. \tag{6}$$

Integrating Eq. (1), at the near-surface inflow streamtube, from large radius (∞) to the center (0) of the dust devil (see Fig. 1), we get

$$\int_\infty^0 \alpha \, dp \approx \int_\infty^0 \mathbf{f} \cdot d\mathbf{l}, \tag{7}$$

where we have neglected changes in kinetic and potential energy of air parcels moving toward the center of the dust devil. Our justification for neglecting changes in kinetic and potential energy is that, near the surface, there is a stagnation point at the center of the dust devil (relative to the dust devil motion), and that to a first approximation the surface is flat. Equation (7) relates the surface radial pressure drop to the near-surface frictional loss of energy. The notation $\int_\infty^0$ indicates an integral from ∞ to 0, throughout the inflow streamtube, normalized by the streamtube's mass.

Using the ideal gas law to eliminate α, Eq. (7) becomes

$$\int_\infty^0 RT \, d \ln p \approx \int_\infty^0 \mathbf{f} \cdot d\mathbf{l}, \tag{8}$$

where R is the specific gas constant for air.

Defining the fraction of the total dissipation of mechanical energy consumed by friction at the surface as

$$\gamma \equiv \frac{\int_\infty^0 \mathbf{f} \cdot d\mathbf{l}}{\int_m \mathbf{f} \cdot d\mathbf{l}}, \tag{9}$$

we get

$$\int_\infty^0 RT \, d \ln p \approx \gamma \int_m \mathbf{f} \cdot d\mathbf{l}.$$

Using Eq. (5) to eliminate $\int_m \mathbf{f} \cdot d\mathbf{l}$, we get

$$-\int_\infty^0 RT \, d \ln p \approx \gamma \int_m T \, ds, \tag{10}$$

where $\int_m T \, ds$ is the net heat input into the dust devil convective heat engine. The net heat input, in turn, is the amount of heat which is turned into work. Since the thermal efficiency η of a heat engine is defined as the fraction of the heat input that is turned into work, we have that

$$\eta \equiv \frac{\int_m T \, ds}{\int_\infty^0 T \, ds}, \tag{11}$$

where $\int_\infty^0 T \, ds$ is the heat input into the dust devil. Using Eq. (11) to eliminate the net heat input $\int_m T \, ds$ in Eq. (10), we get

$$-R\overline{T_s}\,\ln\frac{p_0}{p_\infty} \approx \gamma\eta\int_\infty^0 T\,ds, \tag{12}$$

where $\overline{T_s}$ is the mean temperature of the surface-layer air, that is the mean temperature at which heat is absorbed by the dust devil heat engine. The overbar represents a horizontal average from ∞ to 0. Equation (12) states that the surface pressure drop from large radius (∞) to the center (0) of the dust devil is proportional to the net heat input. Therefore, the net work performed by the dust devil heat engine on its environment is proportional to the surface pressure drop.

It follows from the first law of thermodynamics and the ideal gas law that

$$T\,ds = d(c_pT + L_vr) - RT\,\ln p. \tag{13}$$

Neglecting changes in the heat capacity of air and in the latent heat of vaporization of water, we get

$$T\,ds \approx c_p dT + L_v dr - RT\,\ln p. \tag{14}$$

Integrating Eq. (14) from large radius toward the center of the dust devil, we get an expression for the heat input, that is

$$\int_\infty^0 T\,ds \approx \int_\infty^0 (c_p\,dT + L_v\,dr) - \int_\infty^0 RT\,d\,\ln p$$

$$\approx c_p(T_0 - T_\infty) + L_v(r_0 - r_\infty) - R\overline{T_s}\,\ln\frac{p_0}{p_\infty}. \tag{15}$$

Substituting Eq. (15) into Eq. (12), we get

$$-R\overline{T_s}\,\ln\frac{p_0}{p_\infty} \approx \gamma\eta\left[c_p(T_0 - T_\infty) + L_v(r_0 - r_\infty) - R\overline{T_s}\,\ln\frac{p_0}{p_\infty}\right]$$

$$p_0 \approx p_\infty \exp\left\{\left(\frac{\gamma\eta}{\gamma\eta - 1}\right)\left[\left(\frac{c_p}{R}\right)\left(\frac{T_0 - T_\infty}{\overline{T_s}}\right) + \left(\frac{L_v}{R}\right)\left(\frac{r_0 - r_\infty}{\overline{T_s}}\right)\right]\right\}. \tag{16}$$

Since most of the heat input to a dust devil is in the form of sensible heat flux, we can neglect changes in the air parcel's water vapor content. (Note that this term is the most important in waterspouts and tornadoes.) Thus, the radial pressure drop across a dust devil is given by

$$\Delta p \equiv (p_\infty - p_0)$$

$$\approx p_s\left\{1 - \exp\left[\left(\frac{\gamma\eta}{\gamma\eta - 1}\right)\left(\frac{1}{\chi}\right)\left(\frac{T_0 - \overline{T_s}}{\overline{T_s}}\right)\right]\right\}, \tag{17}$$

where $\chi \equiv R/c_p$ (we have assumed $T_\infty \approx \overline{T_s}$ and $p_\infty \approx p_s$). The net work performed by the dust devil convective heat engine is proportional to the radial pressure drop across the dust devil [see Eq. (12)]. Therefore, the radial pressure drop provides a good measure of the dust devil intensity.

Equation (17) is general; that is, it applies to either rotating or nonrotating convective plumes. Therefore, Eq. (17) can be used to estimate the near-surface pressure depression within any dry convective plume (or to any moist convective plume if the latent heat term is included). Interestingly, Eq. (17) predicts that the intensity of a convective vortex increases with increases in the fraction of the total dissipation of mechanical energy occurring near the surface. This might provide an explanation for the smallness of the pressure drop across nonrotating convective plumes.

It follows from Eq. (17) that the intensity of dust devils depends on the surface air temperature increase from the local environment toward the center of the dust devil. The daytime surface air temperature over a desert is regulated mainly by sensible heat flux from the ground into the surface air. The sensible heat flux, in turn, is proportional to the difference between the ground temperature and the surface air temperature (see the bulk aerodynamic formula). Therefore, the ground temperature provides an upper bound (through the second law of thermodynamics) for the temperature at the center of a dust devil, T_0 (assuming an equal mass contribution from warmer and colder air parcels, strong mixing near the surface reduces the difference between the center air temperature and the ground temperature to ~50% of its maximum possible value).

A large air temperature increase is likely to occur when air parcels sitting over relatively cold surfaces move toward warmer surfaces. Therefore, dust devils are more likely to form in regions of larger horizontal temperature gradients (within the dust devil inflow region, that is ~100 m) than in regions of smaller temperature gradients. This idea is supported by the observation of a local maximum of dust devil occurrence near dry washes (Sinclair 1966) and over dry fields downwind of irrigated fields (G. Osoba 1997, personal communication). Moreover, it is supported by the occasional observation of dust devils in the French countryside during the summer, over warm fields with cooler surroundings (Georgii 1952). Obviously, we are making the hypothesis that the observation of larger dust devil occurrence near dry washes is due to temperature contrasts between areas of sandy soil and areas covered by vegetation, which frequently occur around dry washes. However, the reader should be warned that the more

frequent observation of dust devils around dry washes might also be due to the presence of a larger quantity of dust (fine soil) near dry washes. A large quantity of dust near dry washes would potentially make visible dust devils that would elsewhere be invisible. Our hypothesis is supported by observations that dust devil occurrence is *not* as frequent in plain desert land covered by loose materials as it is near dry washes. We plan to test our hypothesis by making careful observations of dust devil occurrence as well as temperature measurements around dry washes and plain desert land covered by loose materials.

Equation (17) also predicts that the intensity of a dust devil is a function of its thermodynamic efficiency. The thermodynamic efficiency of the convective heat engine can be written as

$$\eta = \frac{T_h - T_c}{T_h}, \tag{18}$$

where T_h and T_c are, respectively, the entropy averaged temperatures of the heat source and sink. To a first approximation, the temperature of the heat source of the dust devil convective heat engine is equal to the average temperature of the surface air $T_h \approx \overline{T_s}$ (Rennó and Ingersoll 1996). To a first approximation, the entropy of the convective boundary layer is constant with height. Therefore, the entropy averaged temperature of the boundary layer air is equal to its pressure averaged temperature. It follows from the first law of thermodynamics that the temperature profile of a dry adiabatic layer is given by

$$T \approx \overline{T_s}\left(\frac{p}{p_s}\right)^{\chi}. \tag{19}$$

Integrating Eq. (19) from the surface to the top of the convective layer, we get an expression for the temperature of the heat sink

$$\begin{aligned} T_c &= \frac{\overline{T_s}(p_s^{\chi+1} - p_{\text{top}}^{\chi+1})}{(p_s - p_{\text{top}})(\chi + 1)p_s^{\chi}}, \\ &= b\overline{T_s}, \end{aligned} \tag{20}$$

where p_s is the ambient surface pressure, p_{top} is the ambient pressure at the top of the convective boundary layer, and b is defined as

$$b \equiv \frac{(p_s^{\chi+1} - p_{\text{top}}^{\chi+1})}{(p_s - p_{\text{top}})(\chi + 1)p_s^{\chi}}. \tag{21}$$

It follows from Eqs. (18) and (20) that the thermodynamic efficiency of a dry convective heat engine is given by

$$\begin{aligned} \eta &\approx \frac{\overline{T_s} - b\overline{T_s}}{\overline{T_s}} \\ &\approx 1 - b. \end{aligned} \tag{22}$$

Equation (22) states that the thermodynamic efficiency of a dust devil, or of any dry convective heat engine, is a function of the pressure thickness of the convective layer. This result is in agreement with observations of boundary layer convection and results of numerical simulations that show an increase in the intensity of convection with increases in the boundary layer thickness (Deardorff 1970).

Defining the horizontal thermodynamic efficiency of the dust devil as

$$\eta_H \equiv \frac{T_0 - \overline{T_s}}{\overline{T_s}}, \tag{23}$$

Eq. (17) becomes

$$\Delta p \approx p_s\left\{1 - \exp\left[\left(\frac{\gamma\eta}{\gamma\eta - 1}\right)\left(\frac{\eta_H}{\chi}\right)\right]\right\}. \tag{24}$$

Note that since, in general, for boundary layer convection $\gamma\eta \ll 1$, to a first approximation $(\gamma\eta - 1) \approx -1$. It follows from Eq. (24) that the potential intensity of dust devils (Δp) is a function of the surface pressure, the ''vertical thermodynamic efficiency'' (or the pressure thickness of the convective layer), the near-surface fraction of the mechanical dissipation of energy, and the horizontal thermodynamic efficiency.

Assuming that, to a first approximation, dust devils are in cyclostrophic balance, Eq. (24) can be used for the computation of wind speed around dust devils. An atmospheric vortex in cyclostrophic balance satisfies the equation

$$\frac{v^2}{a} \approx \alpha\left(\frac{\Delta p}{a}\right), \tag{25}$$

where v is the tangential wind speed around the vortex, and a is the vortex radius (the radius of maximum wind).

Substituting Eq. (25) into Eq. (24), and using the ideal gas law, we get an expression for the wind speed around a dust devil:

$$v \approx \sqrt{R\overline{T_s}\left\{1 - \exp\left[\left(\frac{\gamma\eta}{\gamma\eta - 1}\right)\left(\frac{\eta_H}{\chi}\right)\right]\right\}}. \tag{26}$$

Equation (26) suggests that the wind speed around a dust devil does not explicitly depend on its size. That is, the magnitude of the tangential wind speed depends only on the value of the pressure depression. The value of pressure depression, in turn, depends only on the thermodynamics of the convective plume associated with the dust devil. However, the wind speed around a dust devil might depend on its size through its horizontal thermodynamic efficiency, which, in turn, might increase with the dust devil size.

The magnitude of the vertical component of the wind velocity within the dust devil can be computed by Eq. (42) of Rennó and Ingersoll (1996), that is

$$w \approx \sqrt{\left(\frac{c_p}{8\epsilon\sigma_R T_c^3}\right)\frac{\eta F_{\text{in}}}{\mu}}, \tag{27}$$

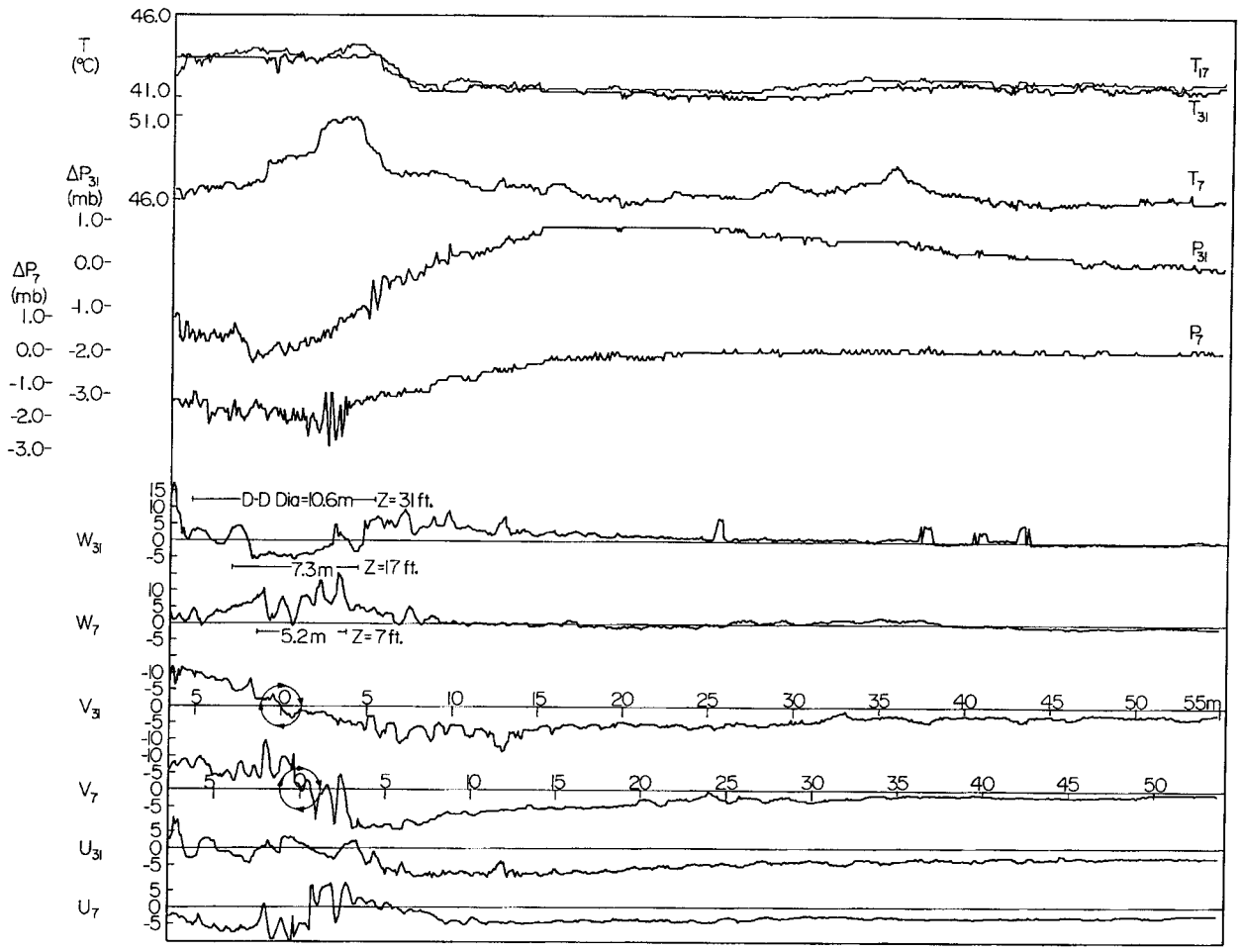

FIG. 2. Horizontal profiles of temperature (°C), pressure (mb), and the three cylindrical components of the wind velocity (m s^{-1}) through the base of a dust devil, at 7, 17, and 31 ft above the surface. The measurements were made by Sinclair (1966) near Tucson, Arizona, over flat terrain on 13 August 1962 at 1300 UTC (after Sinclair 1966).

where $\epsilon \approx 0.7$ is the emissivity of the boundary layer air, $\sigma_R \approx 5.67 \times 10^{-8}$ W m^{-2} K^{-4} is the Stefan–Boltzmann constant, F_{in} is the heat input to the convective heat engine, and μ is a dimensionless coefficient of turbulent dissipation of mechanical energy. To estimate μ we must know both the length of the convective path (that is of the convective circulation) and the length and velocity scale of the most energetic eddies (Rennó and Ingersoll 1996). Since in homogeneous and isotropic turbulence the most energetic eddies are the largest, we arbitrarily assume that the most energetic eddies have the length and velocity scale of the convective drafts. Assuming that the length of the convective path is between 2 and 8 times the thickness of the convective layer, we get $\mu \approx 10$–50.

Figure 2 displays the profiles of temperature (°C), pressure (mb), and the three cylindrical components of the wind velocity (m s^{-1}) through the base of a dust devil, at 7, 17, and 31 ft above the surface. The measurements were made by Sinclair (1966) near Tucson, Arizona, over flat terrain on 13 August 1962 at 1300 MST (Sinclair 1973). It follows from Sinclair's observations that $T_\infty \approx 319$ K, $T_0 \approx 324$ K, $\Delta p \approx 3.0$ hPa, and that both the tangential (v) and vertical wind (w) speed fluctuate between 10 and 15 m s^{-1}. The heat input to a dry convective system is approximately equal to the surface sensible heat flux; its typical summertime value at the desert around Tucson at 1300 MST is $F_{\text{in}} \approx 455$ W m^{-2}.

Taking $\overline{T_s} \approx T_\infty \approx 319$ K, $T_0 \approx 324$ K, and assuming typical summertime values for the surface pressure $p_s \approx p_\infty \approx 925$ hPa and the pressure at the top of the dust devil convective plume, 650 hPa, we get $\eta \approx 0.050$, $\eta_H \approx 0.016$. Assuming dry air, we have that $c_p \approx 1005$ J kg^{-1} K^{-1} and $\chi \approx 0.286$. Taking $\gamma \approx 0.5$–1.0 and the above numbers, Eqs. (24), (26), and (27) give $\Delta p \approx 1.3$–2.7 hPa, $v \approx 11$–16 m s^{-1}, and $w \approx 8$–16 m s^{-1}. These numbers are close to the observed values, hence supporting our theory. Moreover, they suggest that most of the mechanical dissipation of energy occur near the surface.

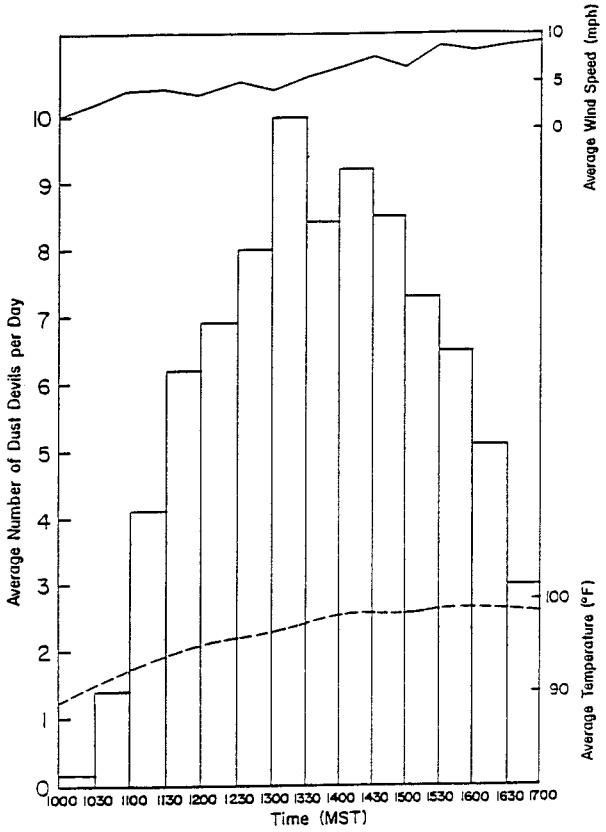

FIG. 3. Diurnal variation of dust devil occurrence for the Avra Valley based on the observation of 1663 dust devils by Sinclair (1966). The solid curve at the top of the figure shows the average surface wind speed (mph) and the dotted curve at the bottom shows the average surface temperature at Ryan Field in the Avra Valley (after Sinclair 1969).

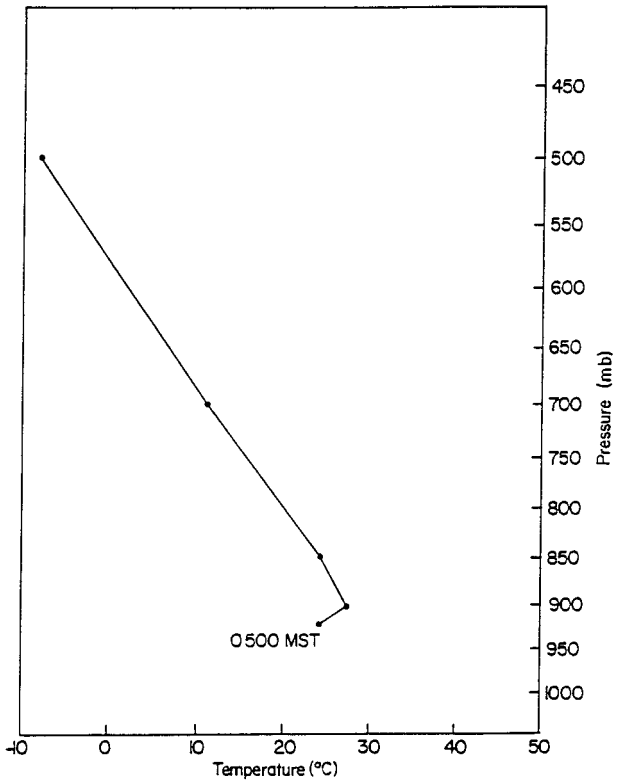

FIG. 4. Sketch of typical early-morning temperature soundings around Tucson (adapted from Sinclair 1969).

3. Diurnal variation of dust devil activity

Assuming that, to a first approximation, convective boundary layers are quasi steady on the timescale of dust devils, we can estimate the diurnal variation of dust devil activity. Multiplying Eq. (6) by the convective mass flux (M), we get

$$M \oint T\, ds = -M \oint \mathbf{f} \cdot d\mathbf{l}. \tag{28}$$

Equation (28) states that, at quasi-steady state, the dust devil activity is such that the flux of mechanical energy made available by the convective heat engine ($F_{\text{av}} = M \oint T\, ds$) is equal to the flux of energy mechanically dissipated by friction ($F_d = -M \oint \mathbf{f} \cdot d\mathbf{l}$). That is, in quasi-steady state

$$F_{\text{av}} \approx \eta F_{\text{in}} \approx F_d, \tag{29}$$

where F_{in} is the heat input to the convective heat engine. To a first approximation, the heat input is equal to the surface sensible heat flux, F_s.

From Eqs. (22) and (29), we get

$$F_{\text{av}} \approx (1 - b)F_s; \tag{30}$$

alternatively, we can write

$$F_{\text{av}} \approx \eta F_s. \tag{31}$$

Equation (30) states that the flux of energy available to drive dust devils (and therefore, the dust devil activity) is proportional to the boundary layer thickness and the sensible heat flux. Equation (31) states that the flux of energy available to drive dust devils is proportional to the thermodynamic efficiency of boundary layer plumes and the sensible heat flux.

Figure 3 displays the diurnal variation of dust devil occurrence for Avra Valley, Arizona, based on the observation of about 1600 dust devils by Sinclair (1966). The solid curve at the top of the figure shows the average surface wind speed (mph) and the dotted curve at the bottom shows the average surface temperature at Ryan Field, in the Avra Valley (Sinclair 1969). Sinclair's observations pose at least two important questions: why is there an abrupt increase in the number of dust devils around 1030–1100 MST, and why does the dust devil activity peak at around 1300 MST? We use Eq. (30) to address these two questions.

Figure 4 displays a sketch of typical early-morning temperature soundings around Tucson. A temperature inversion extending from the surface to a few hundred meters above it often occurs due to overnight heat loss

TABLE 1. Predicted energy flux available to drive dust devils (F_{av}) in typical summertime days around Tucson, Arizona. The values were computed with Eq. (22) using data from a typical early-morning temperature sounding around Tucson and observed diurnal variation of the surface sensible heat flux for a southwest desert region (Sellers 1965).

Time	η (adm)	F_S (W m^{-2})	F_{av} (W m^{-2})
1000 MST	0.01	225	2
1100 MST	0.01	320	3
1200 MST	0.05	420	21
0100 MST	0.05	455	23
0200 MST	0.05	440	22
0300 MST	0.05	320	16
0400 MST	0.05	270	14
0500 MST	0.05	55	3
0600 MST	0.05	0	0

by radiation. After sunrise, the surface is warmed by solar radiation, and hot air parcels rise until they become colder than their environment. The thermodynamic efficiency of these early-morning convective plumes is very small (≤ 0.01) because they are very shallow [see Eq. (22)]. These weak convective plumes will continue until the surface temperature is large enough to produce convective plumes that can break through the inversion layer (this typically occurs at around 1100 MST). Further temperature increases will rapidly cause the depth of the convective plumes to increase to a few thousand meters. This, in turn, will produce an abrupt increase in the thermodynamic efficiency of convective plumes and dust devils.

The energy flux available to drive convective plumes and dust devils is proportional to the product of their thermodynamic efficiency with the heat input (the nonconvective surface heat flux). For dry convective plumes, the heat input is approximately equal to the surface sensible heat flux.

Table 1 shows the predicted flux of energy available to drive dust devils in typical summertime days around Tucson, Arizona. The values displayed in Table 1 were computed with Eq. (22), using data from a typical early-morning temperature sounding around Tucson and observed diurnal variation of the surface sensible heat flux (Sellers 1965). The calculations based on our theory explain both the abrupt increase in dust devil occurrence around 1100 MST and the time of peak dust devil occurrence. The rapid increase in dust devil occurrence at around 1100 MST is due to an abrupt increase in the efficiency of thermal plumes. The peak in the dust devil occurrence at around 1300 MST is due to a peak in the surface heat input at a time of thermodynamically efficient (deep) convective plumes.

4. Conclusions

We present a scaling theory for dust devils that provides a simple physical interpretation for their intensity, diurnal variation in occurrence, and potential spatial distribution. Our theory was successfully tested against observations of dust devils around Tucson, Arizona. It predicted the correct pressure depression, wind velocity, and the diurnal variation in the occurrence of dust devils. We are currently applying our scaling theory to waterspouts and tornadoes with encouraging results.

Our theory predicts that the potential pressure depression between the center of a dust devil and its environment is a function only of the ambient thermodynamic variables. Thus, given the environmental conditions, the potential pressure depression of a dust devil is a known variable. Since dust devils receive their vorticity from ambient wind shears, our theory suggests that their radius must be determined by the initial angular momentum of air parcels converging toward their center. That is, the tangential velocity of air parcels converging toward the center of a dust devil increase, but only up to a point where the dust devil pressure depression can still maintain a cyclostrophic balance. Then, the farther movement of air parcels toward the center of the dust devil would produce an unbalanced centrifugal force that would drive the air parcels away from the dust devil center (an expansion of the dust devil region of maximum tangential wind). The above hypothesis suggests that ambients of stronger horizontal wind shears lead to larger dust devils than ambients of smaller wind shears. This conclusion is supported by observations that dust devil diameters are biased toward large values in environments of high wind speed, and therefore large horizontal wind shears (Sinclair 1966).

Acknowledgments. We would like to thank The University of Arizona's Department of Atmospheric Sciences for supporting this study and The University of Arizona's NASA Space Grant Undergraduate Research Internship Program for partially supporting the two coauthors. We also would like to thank Ms. Margaret S. Rae, Dr. Maria Carmen Lemos, Prof. R. Schotland, Prof. Howard Bluestein, and Dr. John Leibacher for reading the manuscript and making many useful suggestions. Finally, we would like to thank Prof. George Craig and two anonymous reviewers for their suggestions and helpful criticisms that substantially improved the original paper. In particular, one of the anonymous reviewers called our attention to the fact that the neglect of changes in potential and kinetic energy in Eq. (5) is justified by the fact that, at the surface, there is a stagnation point at the center of the vortex.

REFERENCES

Battan, L. J., 1958: Energy of a dust devil. *J. Meteor.*, **15,** 235–237.
Brunt, D., 1941: *Physical and Dynamical Meteorology.* Cambridge University Press, 428 pp.
Carroll, J. J., and J. A. Ryan, 1970: Atmospheric vorticity and dust devil rotation. *J. Geophys. Res.*, **20,** 5179–5184.
Davies-Jones, R. P., 1984: Streamwise vorticity: The origin of updraft rotation in supercell storms. *J. Atmos. Sci.*, **41,** 2991–3006.
Deardorff, J. W., 1970: Convective velocity and temperature scales

for the unstable planetary boundary layer and for Rayleigh convection. *J. Atmos. Sci.,* **27,** 1211–1212.

Emanuel, K. A., 1986: An air–sea interaction theory for tropical cyclones. Part I: Steady-state maintenance. *J. Atmos. Sci.,* **43,** 585–604.

Fiedler, B. H., and R. Rotunno, 1986: A theory for the maximum windspeed in tornado-like vortices. *J. Atmos. Sci.,* **43,** 2328–2340.

Flower, W. D., 1936: Sand devils. U.K. Meteorological Office Tech. Note 5, No. 71, 16 pp.

Georgii, W., 1952: The meteorological basis of soaring. U.S. Naval Ordinance Test Station Tech. Memo. NOTS TM-258, 122 pp.

Grant, C. C., 1949: Dust devils in the subartic. *Weather,* **4,** 402–403.

Haltiner, G. J., and F. L. Martin, 1957: *Dynamical and Physical Meteorology.* McGraw-Hill, 470 pp.

Ives, R. L., 1947: Behavior of dust devils. *Bull. Amer. Meteor. Soc.,* **28,** 168–174.

Kaimal, J. C., and J. A. Businger, 1970: Case studies of a convective plume and a dust devil. *J. Appl. Meteor.,* **9,** 612–620.

Lilly, D. K., 1982: The development and maintenance of rotation in convective storms. *Intense Atmospherics Vortices: Topics in Atmospheric and Oceanographic Sciences,* Springer-Verlag, 149–160.

Rennó, N. O., and A. P. Ingersoll, 1996: Natural convection as a heat engine: A theory for CAPE. *J. Atmos. Sci.,* **53,** 572–585.

Rotunno, R., and J. B. Klemp, 1985: On the rotation and propagation of simulated supercell thunderstorm. *J. Atmos. Sci.,* **42,** 271–292.

Ryan, J. A., and J. J. Carroll, 1970: Dust devil wind velocities: Mature state. *J. Geophys. Res.,* **75,** 531–541.

Sellers, W. D., 1965: *Physical Climatology.* University of Chicago Press, 272 pp.

Simpson, J., B. R. Morton, M. C. McCumber, and R. S. Penc, 1986: Observations and mechanisms of GATE waterspouts. *J. Atmos. Sci.,* **43,** 753–782.

Sinclair, P. C., 1966: A quantitative analysis of the dust devil. Ph.D. dissertation, The University of Arizona, 292 pp.

——, 1969: General characteristics of dust devils. *J. Appl. Meteor.,* **8,** 32–45.

——, 1973: The lower structure of dust devils. *J. Atmos. Sci.,* **30,** 1599–1619.

Wegener, A., 1914: Staubwirbel auf Island. *Meteor. Z.,* **31,** 199 pp.

Williams, N. R., 1948: Development of dust and similar scale vortices. *Bull. Amer. Meteor. Soc.,* **29,** 106–117.